Space-charge anomalies in insulators caused by non-local impact ionisation

1989 J. Phys.: Condens. Matter 1 7021

(http://iopscience.iop.org/0953-8984/1/39/013)

J. Phys.: Condens. Matter 1 (1989) 7021–7031. Printed in the UK

Space-charge anomalies in insulators caused by non-local impact ionisation

B K Ridley and F A El-Ela
Department of Physics, University of Essex, Colchester CO4 3SQ, UK

Received 28 March 1989

Abstract. The non-local nature of impact ionisation is modelled using lucky-drift theory with the assumption that the relevant electric field is the average field, but that the relevant drift velocity is that associated with the local field. The carrier density relevant for impact ionisation is also taken to be non-local. The model is applied to the case of a thin film insulator with Fowler–Nordheim injections of electrons at the cathode. For clarity's sake, we avoid considering the excitation of holes and limit attention to the ionisation of a set of occupied deep-level states present in high concentration. Further simplifying assumptions include the neglect of diffusion, overshoot and non-parabolicity. We show that the non-local nature of the ionisation process reduces the local field markedly, resulting in a pile-up of free electrons to maintain current continuity in the rest of the film. This is contrasted with the prediction of local impact ionisation theory, in which the field is reduced merely to that necessary to sustain a small level of ionisation. Under certain circumstances space-charge striations are produced—this is analogous to the situation in gas discharge—and for some film thicknesses a negative differential resistance occurs.

1. Introduction

The importance of non-local effects in impact ionisation has been long recognised, particularly in connection with breakdown in gases, where Crooke's dark space and glow striations provide classic examples. Basically the point is that impact ionisation at a local z in an electric field $\mathscr{E}(z)$ is a consequence of electrons drifting down the potential gradient upstream of the location z, say from z_0, picking up an energy E given by

$$E = \int_{z_0}^{z} e\mathscr{E}(z)\,\mathrm{d}z \tag{1}$$

where $E \geqslant E_I$, the threshold energy (as determined by conservation of momentum and energy). The ionisation rate, $W_I(z)$, is therefore a function of the carrier density $n(z_0)$, and the average field, $\bar{\mathscr{E}}(z, z_0)$. Where carrier density and field vary with distance non-local effects may become of crucial importance.

Even in the uniform case, impact ionisation rates are notoriously difficult to calculate. Typically, electrons must reach energies of one or more electron volts and only a few need do this, and so only the extreme tail of the distribution function is involved. This was first calculated numerically by Baraff (1962) for electrons in semiconductors, but with the assumption that only the local field was the determining factor. In addition the carrier density was assumed to be uniform, the energy band parabolic, and the threshold

0953-8984/89/397021 + 11 $02.50

was, after some analysis, estimated to be 'hard'. The'effect of dark space on Baraff's theory was discussed by Okuto and Crowell (1974), and more recently the complexity of band structure has been introduced via Monte Carlo simulation by Shichijo and Hess (1981). A simpler approach was offered by lucky-drift theory (Ridley 1983, Burt 1985) in which the probability of impact ionisation was directly related to the probability that a ballistic or drifting electron avoided energy relaxation. It has been shown that the introduction of soft thresholds (low probability of impact ionising at threshold compared with that for relaxing energy) into lucky-drift theory gives excellent agreement with experiment (Ridley 1987, Marsland 1987). Non-local effects in junctions were discussed using lucky-drift theory by Childs (1987).

It is clear that if dark-space effects are ignored, the overall impact ionisation rate will be overestimated. However, it is also true that where the electric field reduces sharply impact ionisation will be underestimated if non-local effects are not taken into account. It is one consequence of this latter point that we wish to explore in this paper, in the context of the impact ionisation of a deep-level defect in an insulator when the electrons are injected from the cathode via Fowler–Nordheim (FN) tunnelling. This context is of importance to the understanding of electrical breakdown in insulators and electroluminescence in large-gap semiconductors. We wish to show that the ionisation of defects leads to space-charge anomalies, which are direct consequences of non-local effects. These anomalies, in turn, produce a spatial distribution of field markedly different from that predicted by local-field theory, and this has profound implications for the interpretation of experimental data. Under certain circumstances a spatial oscillation of the field occurs; this is analogous to the striations commonly observed in gas discharge. This in turn can give rise to a current-controlled negative differential resistance (NDR) for some ranges of film thickness.

2. The physical model

We consider a thin film of a large-band-gap semiconductor or an insulator in which there is a high concentration (10^{18}–10^{20} cm^{-3}) of deep-level defects containing electrons. A voltage V is applied across the film that is large enough for a current of electrons to be injected at the cathode $z = 0$ by FN tunnelling. We will assume that the holes are not injected at the anode, and that nor are they excited in the film by impact ionisation. Our model is therefore a single-carrier one. For simplicity we regard the electron band structure to be free-electron-like, i.e. parabolic, with the effective mass equal to the free-electron rest mass, and spherical. Such a band structure approximately reflects the true band structure in an extended-zone scheme. We also regard the scattering proceses involving electrons and phonons to be modelled by non-polar inter-valley scattering with a rate proportional to the density of final states and independent of the degree of Umklapp involved. In this we are merely extrapolating the known situation in, say, silicon to the situation at high energies, regarding all forms of polar scattering as being ineffective at high carrier energies. Since, mostly, large-wavevector phonons will be involved we have adopted an Einstein model and assumed a common frequency ω. Thus our scattering rate is proportional $E^{1/2}$, where E is the energy, which is appropriate to high-frequency phonons for which the interaction strength is proportional to optical strain. (The assumption made by Sparks *et al* (1981), and subsequently by Fischetti *et al* (1985), that the interaction is proportional to acoustic strain, giving a rate proportional to $E^{3/2}$, is inconsistent with their own assumption that zone-edge (i.e. inter-valley)

phonons are involved. The latter have a zero-order deformation interaction with electrons proportional to optical strain and only a first-order interaction proportional to acoustic strain. Moreover, the latter is proportional to the wavevector of the phonon and this cannot physically exceed its value at the zone boundary. It is apparently by taking the phonon wavevector to be unrestricted in magnitude in Umklapp processes that gives rise to the extra factor of E in this approach.)

Injection is modelled by FN tunnelling (Nordheim 1928, Burgess and Kroemer 1953) with a band-edge effective mass of 0.27 m_0 (the value for ZnS), i.e.

$$J = A(\mathscr{E}_0)\mathscr{E}_0^2 \exp(-B(\mathscr{E}_0)\varphi^{3/2}/\mathscr{E}_0) \tag{2}$$

where $A(\mathscr{E}_0)$, $B(\mathscr{E}_0)$ are slowly varying functions of the cathode field $\mathscr{E}_0$, and φ is the barrier height at zero field.

Impact ionisation is modelled by soft-threshold lucky-drift theory. For band-to-band excitation that rate of ionisation near threshold is given by the expression (Keldysh 1960, Ridley 1987)

$$1/\tau_I = (p_0/\tau_E(E_I))[(E - E_I)/E_I]^2 \tag{3}$$

where p_0 is the soft threshold factor and $\tau_E(E_I)$ is the energy relaxation time at threshold. For GaAs and InP, $p_0 \simeq 1$, and we will take this as a guide. The square of the energy difference arises as a consequence of the increase in available states for both electrons and holes as the energy increases above threshold. For impact ionisation of a deep-level we take the energy dependence to be linear rather than quadratic, since now only one set of states increases in density, namely

$$1/\tau_I = (p_0/\tau_E(E_I))(E - E_I)/E_I. \tag{4}$$

The form of the energy dependence is consonant with that expected on classical grounds (Woods 1987). This rate must be proportional to the density of electrons n_T in the trap, and thus the soft-threshold factor must be proportional to n_T. We will assume that

$$p_0 = n_T/N_0 \tag{5}$$

taking $N_0 = 10^{21}\ \mathrm{cm}^{-3}$, so when $n_T = N_0$, p_0 is of the order of the soft-threshold factor observed in band-to-band ionisation. (This is the equivalent of assuming an ionisation cross section of about $10^{-16}\ \mathrm{cm}^2$.)

In order to include non-local effects we consider the lucky-drift approach. If $P(E)$ is the probability of an electron starting from zero reaching an energy E then

$$P(E) = \exp\left(-\int_0^t \frac{\mathrm{d}t}{\tau_E(E)}\right) = \exp\left(-\int_0^E \frac{\mathrm{d}E'}{e\varepsilon v\tau_E}\right) \qquad (\mathscr{E} > 0) \tag{6}$$

where v is the velocity (group velocity for ballistic electrons, drift velocity for lucky-drift electrons). The probability for impact ionising becomes

$$P_I = \int_{E_I}^{E_{max}} P(E) \exp\left(-\int_{E_I}^{E} \frac{\mathrm{d}E'}{e\mathscr{E}v\tau_I}\right) \frac{\mathrm{d}E}{e\mathscr{E}v\tau_I} \tag{7}$$

with

$$e\mathscr{E}v\tau_I = \begin{cases} (e\mathscr{E}\lambda/rp)E/E_I & \text{ballistic} \\ (e\mathscr{E}\lambda)^2/2rpE_I & \text{drift} \end{cases} \tag{8}$$

and

$$r = \frac{\hbar\omega}{E_I(2n(\omega)+1)} \qquad p = \frac{\tau_E}{\tau_I} = p_0\left(\frac{E}{E_I}\right)^{1/2}\left(\frac{E-E_I}{E_I}\right). \tag{9}$$

P_{LD} is given by lucky-drift theory (Ridley 1987). Here $n(\omega)$ is the phonon occupancy factor. The mean free path λ is related to its value at $T = 0$ K via $\lambda(0) = (2n(\omega)+1)\lambda$.

The dark-space width, z_d, is defined by

$$z_d = E_I/e\bar{\mathscr{E}} \tag{10}$$

where $\bar{\mathscr{E}}$ is the average field. P_I is zero for $z < z_d$, and then increases as E_{max} increases, where

$$E_{max} = e\bar{\mathscr{E}}z \qquad (z > z_d). \tag{11}$$

What matters for both dark space and maximum energy is the average field. Strictly, the field that enters the integral is the local field at energy E, but if this happens to be zero the relation between energy increase and time breaks down. If electrons enter a zero-field region at $z = z_c$ with sufficient energy to produce ionisation, then they will continue to do so for some distance $z - z_c$ depending on the energy relaxation time and the electron velocity. A local field approach would give an impact ionisation rate of zero. To model the continued ability of the electrons to impact ionise we simply choose the field that appears in the integral to be the average field, and not the local field. We may denote this 'the average-field approximation'. This approximation will be valid over distances of order of the energy relaxation length—typically a few hundred ångströms.

In considering the trap kinetics we distinguish the electron density at the cathode, n_c, and the local density n. The rate of change of the trap concentration, neglecting thermal generation and Auger trapping, is

$$dn_T/dt = c(N_T - n_T)n - e_I n_C n_T \tag{12}$$

where e_I is volume ionisation coefficient related to the ionisation coefficient α via

$$e_I n_T = v_d \alpha \tag{13}$$

with α given by lucky-drift theory c is the volume capture coefficient and v_d is the drift velocity.

In situations in which the field drops rapidly at the end of the dark space the average-field approximation will tend to overestimate the ionisation rate, whereas the local field approximation will tend to give a gross underestimate. The former will be a better approximation whenever both the distances involved—dark space and space-charge region—are comparable with the energy relaxation length l_E (typically a few hundred ångströms) or smaller, which is usually the case for trap densities of the order of 10^{18} cm^{-3} and above and typical applied voltages. However, at distances downstream of the space-charge anomaly that are large compared with l_E, the average-field approximation will grossly overestimate the ionisation rate. The problem is that although the available energy is correctly taken into account, the flux of ionising particles is not. As the field drops to the Ohmic region and begins to lower the local drift velocity the flux of ionising particles will weaken and hence the *rate* of ionisation will drop, even though α remains high. To take this effect into account we take the drift velocity that appears in (13) relating the rate to the coefficient as the local drift velocity. This has the effect of drastically reducing the ionisation rate downstream of the space-charge anomaly, which

Table 1. Parameters for the model.

$\varepsilon_s/\varepsilon_0$	$\hbar\omega$	$\lambda(0)$	E_I	c
8.32	33 meV	64 Å	3.0 eV	10^{-10} cm^3 s^{-1}

is more realistic, and also consistent with the basic assumption of lucky-drift theory that the momentum relaxation time, which is the one governing drift velocity, is much shorter than the energy relaxation time. At steady state

$$n_T = cN_T n/(cn + e_T n_C). \tag{14}$$

Non-local effects enter here whenever $n \neq n_c$.

Many substances of interest are GaAs-like, so, for the purpose of modelling low-field effects, we take a drift-velocity–field curve which assumes a light-mass central valley and heavy-mass satellite valleys above it in energy. Electron transfer at high fields leads to a NDR. This is not a needless complication in our case since the NDR does not lead to instability. We therefore assume a particular form for the local drift velocity that is roughly what may be expected for ZnS, namely,

$$v_d = v_s[1 - (1 - 3.25 \times 10^{-5}\,\mathscr{E})\exp(-7.5 \times 10^{-6}\,\mathscr{E})] \tag{15}$$

with $v_s = 5 \times 10^6$ cm s^{-1}. Here, ε is the local field in V cm^{-1}. (This expression is a rough fit to the result of a Monte Carlo simulation for ZnS (El Ela and Ridley 1989).)

The current density, J, is given by our choice of cathode field, whence

$$n_c = J/ev_s. \tag{16}$$

Current continuity demands that, for all z,

$$env_\alpha = J \tag{17}$$

and Gauss's equation determines the variation of the field:

$$\mathrm{d}\mathscr{E}/\mathrm{d}z = (e/\mathscr{E}_s)(N_e - N_{e0}) \tag{18}$$

where

$$N_e = n + N_T \tag{19}$$

and N_{e0} is the electron density required for neutrality. (For convenience $\mathscr{E}$ is taken to be positive if it accelerates electrons in the positive z direction.)

For a given current the calculating procedure was to obtain α from the lucky-drift theory at a given z, calculate n_T using the value of n at $z - \Delta z$, obtain N_e and $\Delta\mathscr{E}$, calculate the local and average fields, obtain n from current continuity, advance to $z + \Delta z$, and repeat. (It was found that it was necessary to take $\Delta z \leqslant 0.1$ Å for $N = 10^{20}$ cm^{-3}.)

3. Results

Table 1 lists the values of parameters chosen, which refer to ZnS as far as they are known.

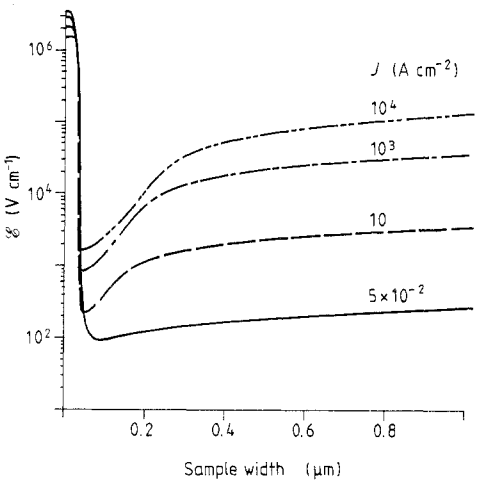

Figure 1. The local-field profile for the current densities shown on the curves for the case $N_T = N_{e0} = 10^{19}$ cm^{-3}.

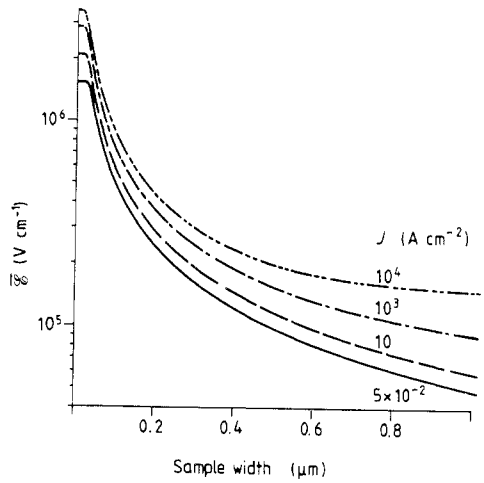

Figure 2. The average-field profile. $N_T = N_{e0} = 10^{19}$ cm^{-3}.

Figure 1 shows the profile at 300 K of the local field for a number of current densities when there are 10^{19} cm^{-3} traps fully occupied by electrons at zero field. The dark space at cathode fields of the order of 10^6 V cm^{-1} for the threshold energy of 3 eV is of the order of 100 Å. Ionisation and subsequent depletion of the traps reduces the field rapidly—the more so the greater the current. A minimum is reached when free electrons build up to keep the current constant, since they replenish the traps, neutralising their positive charge, and add their own negative space charge, which reverses the field gradient. The bigger the current the more rapidly does this occur. The field drops to remarkably low values at the lower currents. There follows a comparatively slow rise, the rate of which is greater the greater the injected density, and there is a trend to a condition of electrical neutrality.

Figure 2 shows the average field. Over the crucial region below 0.1 μm it remains high, though the local field drops dramatically, and continues to encourage impact ionisation and the consequent production of positive space charge. Figure 3 depicts the ionisation coefficient α, which in our model is determined by the average field, the density of free electrons at the cathode, and the local density of trapped electrons. It is zero in the dark space and rises to the point where significant depletion of the traps occurs, at which point the soft-threshold factor reduces and the result is a sharp drop in α. This recovers rapidly as electrons pile up and fill the trap. The notch in figure 3 is thus a consequence of soft-threshold changes at the space-charge anomaly. The volume ionisation rate, e_T, depicted in figure 4, which is the important parameter in the kinetics, does not show this notch since its definition precludes a dependence on trapped electron density. Intense ionisation is confined to a narrow region around 0.04 μm from the cathode. Figure 5 indicates the variation of n_T, the trapped electron concentration, and figure 6 shows the free-electron density profile. The notch in figure 6 is the sole manifestation of the NDR associated with inter-valley transfer. Downstream of the anomaly there is substantial injection. Figure 7 shows the current–voltage characteristic.

The predictions of local field impact ionisation are very different. There is no dark space and the spatial variation of the field is less marked, since no 'overshoot' of

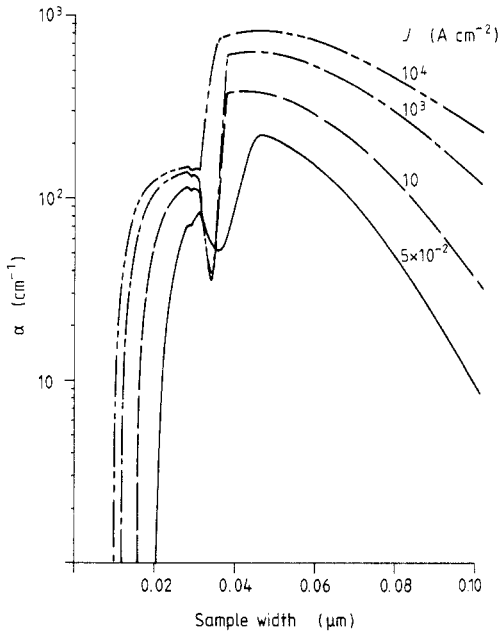

Figure 3. The variation of the ionisation coefficient with distance. $N_T = N_{e0} = 10^{19}$ cm^{-3}.

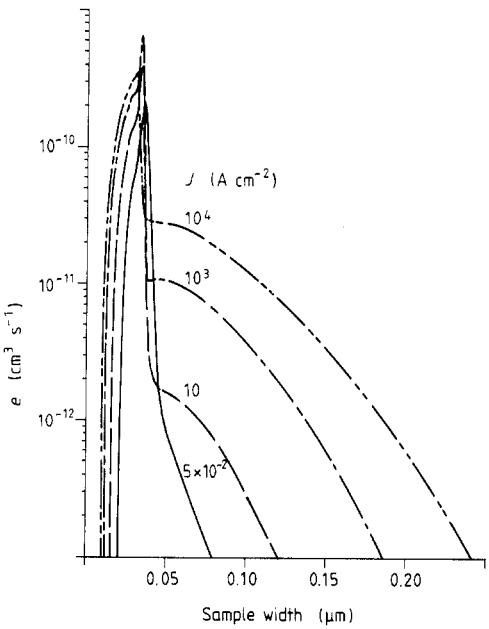

Figure 4. The volume ionisation rate. $N_T = N_{e0} = 10^{19}$ cm^{-3}.

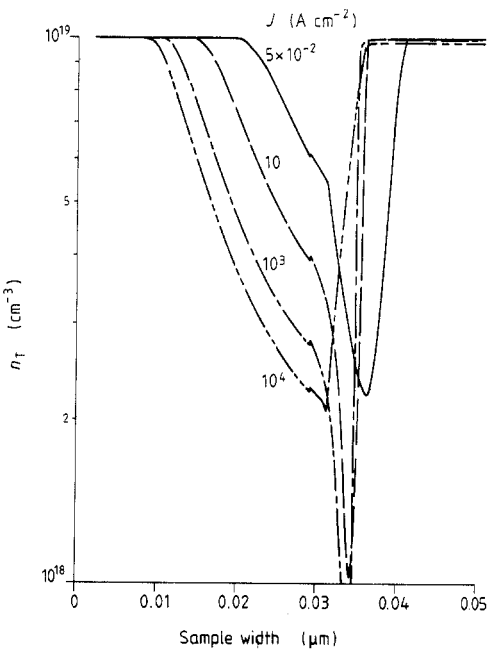

Figure 5. The variation of the trapped electron concentration n_T. $N_T = N_{e0} = 10^{19}$ cm^{-3}.

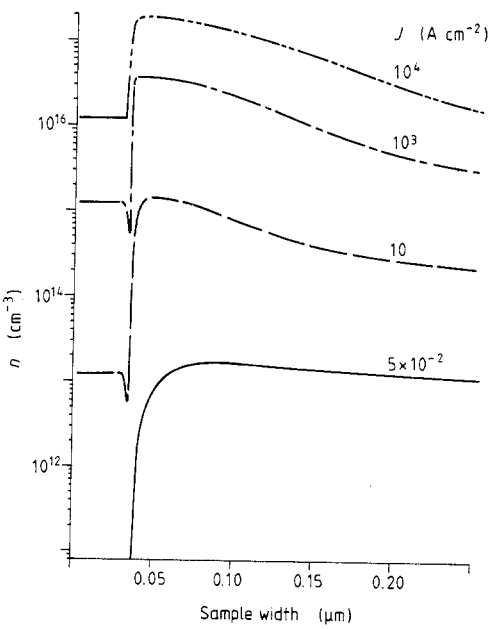

Figure 6. The free-electron density profile. $N_T = N_{e0} = 10^{19}$ cm^{-3}.

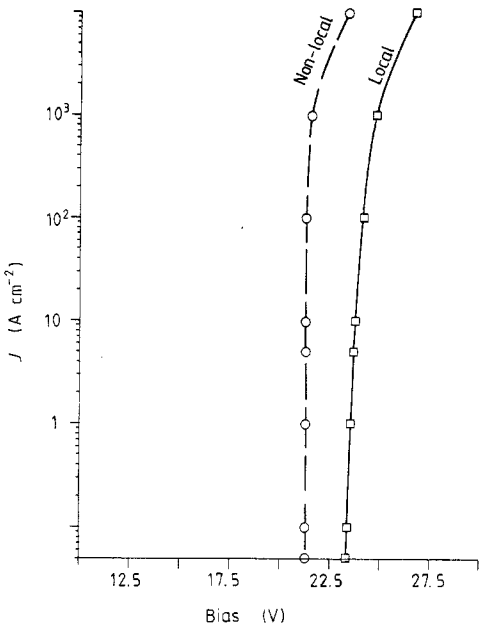

Figure 7. The current–voltage characteristic for 'local field' and 'non-local field' models.

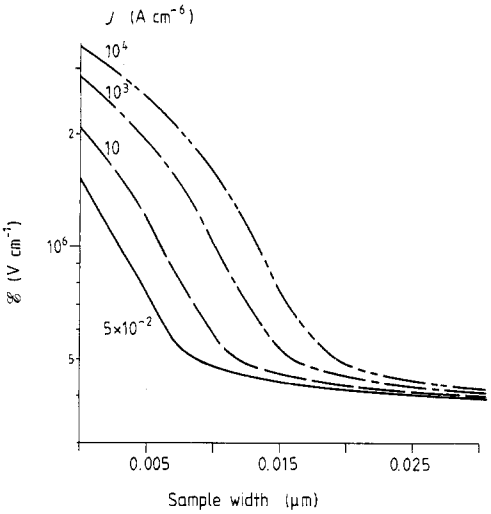

Figure 8. The field profile in the 'local field' model. $N_T = N_{e0} = 10^{19}$ cm^{-3}.

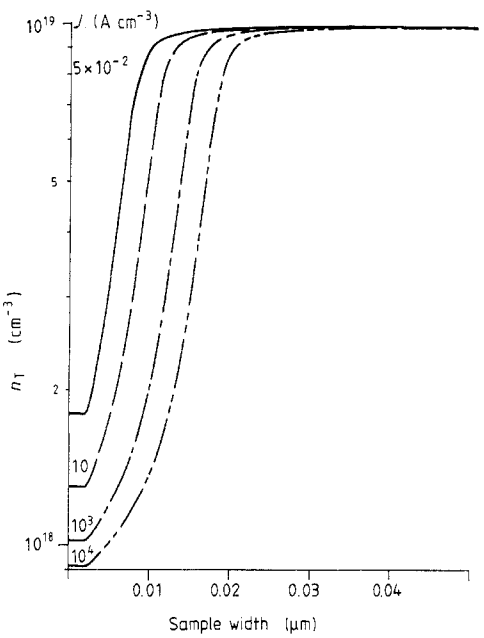

Figure 9. The variation of the trapped electron density in the 'local field' model. $N_T = 10^{19}$ cm^{-3}.

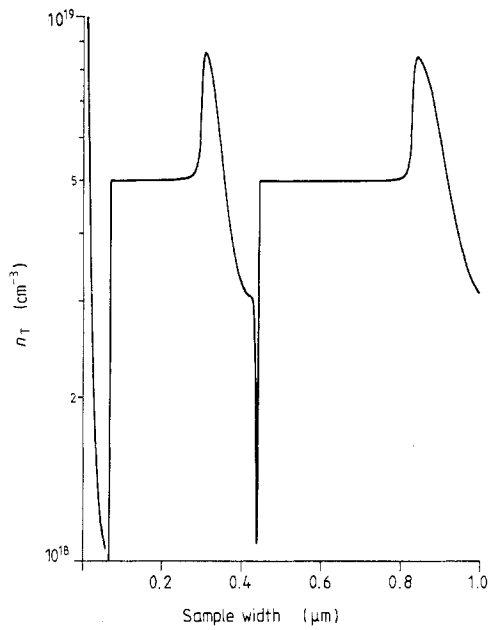

Figure 10. The variation of the trapped electron density in the 'non-local field' model. $N_T = 10^{19}$ cm^{-3}, $N_{e0} = 5 \times 10^{18}$ cm^{-3}, $J = 10$ A cm^{-2}.

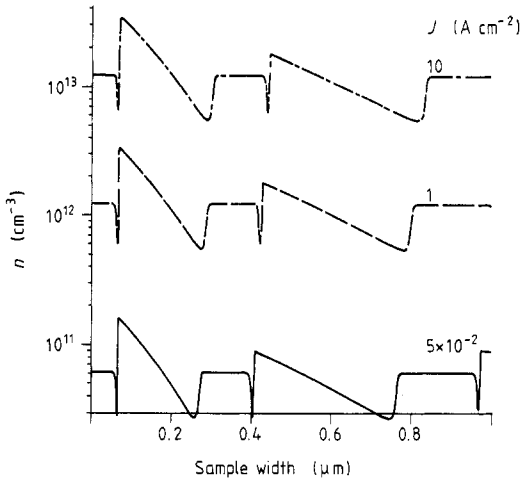

Figure 11. The free-electron density profile. (Conditions as for figure 10.)

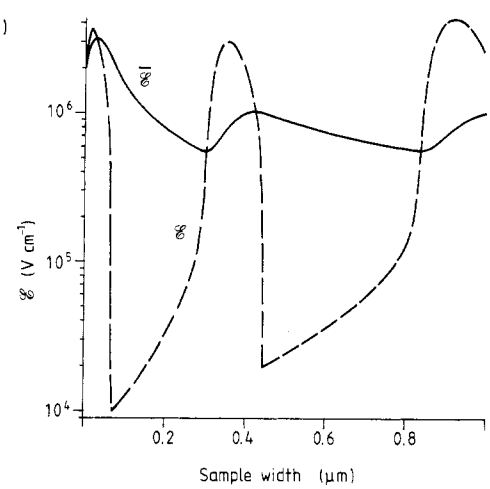

Figure 12. The local field profile and the average-field approximation profile. (conditions as for figure 10.)

ionisation occurs. Figure 8 shows the field variation and figure 9 the trapped electron density variation for the same case as before. The current–voltage curve is that shown in figure 7.

When the deep level is only partially occupied by electrons to begin with the increased potential for capture alters the field profile dramatically. When the field drops and

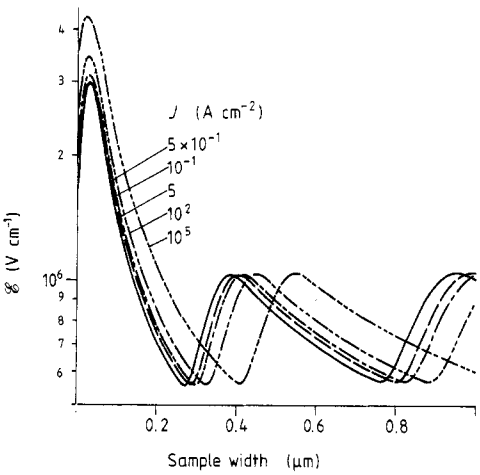

Figure 13. Average-field approximation profiles for the current densities shown on the curves. (Conditions as for figure 10.)

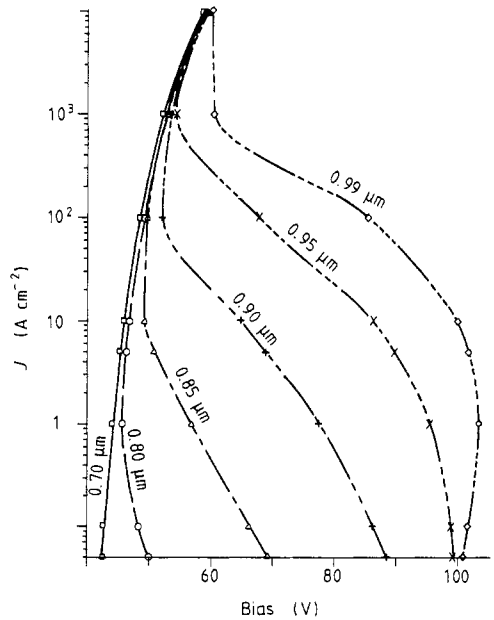

Figure 14. Current–voltage characteristics for $N_T = 10^{19}\,cm^{-3}$, $N_{e0} = 5 \times 10^{18}\,cm^{-3}$ and film thicknesses from 0.7 to 0.09 μm.

ionisation weakens, capture can build up a large negative charge which causes a rapid increase of field to the point where ionisation can again become significant. As a consequence, the profile exhibits spatial oscillations—field striations. The variation of the population of trapped electrons for the case when there are 10^{19} cm^{-3} traps that begin by being half-filled is shown in figure 10 for a current of 10 A cm^{-2}. The corresponding variations of free-electron density and local field are shown in figures 11 and 12. In figure 13 the average-field profile is plotted for a number of current densities. The phase of the oscillations is a function of current density. It follows that for certain thicknesses, e.g. 0.7 μm, the system exhibits a positive differential resistance ($\bar{\mathscr{E}}$ increasing with current density), while for other thicknesses, e.g. 0.9 μm, the system exhibits a NDR (see figure 14). Non-local effects in the impact ionisation of a single partially filled trap thus provides a novel mechanism for current-controlled NDR. This mechanism arises from the varying rapidity with which the space charge produced by ionisation is neutralised and subsequently reversed in sign. At lower currents ionisation is weaker and its effects sooner counteracted.

The striations can be characterised by amplitude, wavelength and phase. Figure 13 shows that the amplitude is virtually independent of current density, the wavelength is about 0.5 μm and the phase shift is about 0.15 μm per 01^7 A cm^{-2}. The wavelength increases as the density of half-filled traps decreases. A more complete study of field striations will be presented soon.

4. Conclusions

We are very conscious of the simplifications inherent in our model. We neglect diffusion and hence overestimate the sharpness of the electron density profile, and we assume that momentum relaxation is instantaneous, and hence we ignore velocity overshoot. The neglected effects would tend to soften the abruptness of the space-charge anomaly, but surely not eliminate it. At such large space-charge densities, with such rapid variations of field, only a Monte Carlo simulation incorporating quantum transport can tackle the physical situation with greater accuracy. In our lucky-drift theory we have assumed average field and average drift velocity to estimate the ionisation coefficient α, but use local drift velocity to obtain the rate, e. We assume parabolic bands in lucky-drift theory yet employ a velocity–field curve that depends upon the existence of upper conduction band valleys, although this is partly justified by their reference to different population groups, namely the impact-ionising cohort for lucky drift, and the thermalised majority for the current. Such inconsistencies may be justified only if their effects are relatively unimportant, and we believe that to be the case here. A more sophisticated treatment is clearly desirable, but the basic physics of the effect—lack of cut-off of impact ionisation due to the non-local element in the mechanism of ionisation and subsequent space-charge anomaly—is, we believe, well illustrated by our simple model.

In conclusion, we have shown that the non-local nature of impact ionisation causes profound space-charge anomalies. In particular we have shown that in the case of impact ionisation of an impurity via electrons injected by Fowler–Nordheim tunnelling, the resulting space-charge anomalies depend on the occupation of the impurity under conditions of electrical neutrality. When the impurity is full the local field exhibits a single striation consisting of a fall from the cathode to a minimum and a subsequent monotonic rise. When the impurity is only partically filled a number of striations occur

in which the local field oscillates spatially with a wavelength dependent on impurity concentration and current. As a result of these striations the system can exhibit current-controlled NDR for certain film thicknesses. This mechanism for NDR requires only a partially filled impurity that can be impact ionised; it is therefore one that is rather commonly encountered.

Acknowledgments

We are indebted to the SERC/DTI for supporting this project and to British Telecom, Martlesham Heath, for the provision of a number of computational facilities.

References

Baraff G A 1962 *Phys. Rev.* **128** 2507
Burgess R E and Kroemer H 1953 *Phys. Rev.* **90** 515
Burt M G 1985 *J. Phys. C: Solid State Phys.* **18** L477
Childs P A 1987 *J. Phys. C: Solid State Phys.* **20** L243
El-Ela F A and Ridley B K 1989 to be published
Fischetti M V, DiMaria D J, Brorson S D, Theis T N and Kirtley J R 1985 *Phys. Rev.* B **31** 8124
Keldysh L V 1960 *Sov. Phys.-JETP* **37** 509
Marsland J 1987 *Solid State Electron.* **30** 125
Nordheim L K 1928 *Proc. Soc.* **121** 626
Okuto Y and Crowell C R 1974 *Phys. Rev.* **102** 369
Ridley B K 1983 *J. Phys. C: Solid State Phys.* **16** 3373
—— 1987 *Semicond. Sci. Technol.* **2** 116
Shichijo H and Hess K 1981 *Phys. Rev.* B **23** 4197
Sparks M, Mills D L, Warren R, Holstein T, Maradudin A A, Sham L J, Loh E and King D F 1981 *Phys. Rev.* B **24** 3519
Woods R C 1987 *IEEE Trans. Electron Devices* **ED-34** 1116